CR-194729

FINAL
IN-35-CR
OCIT
198149
P 7

FINAL TECHNICAL REPORT

1 August 1988 to 31 July 1993

SOLAR IMAGING VECTOR MAGNETOGRAPH

NASA Grant NAGW-1454

to the

University of Hawaii, Institute for Astronomy

2680 Woodlawn Drive, Honolulu, HI 96822

Richard C. Canfield, Principal Investigator

Submitted to

NATIONAL AERONAUTICS AND SPACE ADMINISTRATION

December 15, 1993

N94-21876
Unclas
G3/35 0198149

(NASA-CR-194729) SOLAR IMAGING VECTOR MAGNETOGRAPH Final Technical Report, 1 Aug. 1988 - 31 Jul. 1993 (Hawaii Univ.) 7 p

Introduction

This report describes an instrument which has been constructed at the University of Hawaii to make observations of the magnetic field in solar active regions. Detailed knowledge of active region magnetic structures is crucial to understanding many solar phenomena, because the magnetic field both defines the morphology of structures seen in the solar atmosphere and is the apparent energy source for solar flares.

The new vector magnetograph was conceived in response to a perceived discrepancy between the capabilities of X-ray imaging telescopes to be operating during the current solar maximum and those of existing magnetographs. There were no space-based magnetographs planned for this period; the existing ground-based instruments variously suffered from lack of sensitivity, poor time resolution, inadequate spatial resolution or unreliable sites. Yet the studies of flares and their relationship to the solar corona planned for the 1991-1994 maximum absolutely required high-quality vector magnetic field measurements.

By "vector" measurements we mean that the observation attempts to deduce the complete strength and direction of the field at the measurement site, rather than just the line of sight component as obtained by a traditional longitudinal magnetograph. Knowledge of the vector field permits one to calculate photospheric electric currents, which might play a part in heating the corona; and to calculate energy stored in coronal magnetic fields as the result of such currents. Information about the strength and direction of magnetic fields in the solar atmosphere can be obtained in a number of ways—images of chromospheric fibrils and coronal loops, for example, show structure which appears to be closely related to the magnetic structure—but quantitative data is best obtained by observing Zeeman-effect polarization in solar spectral lines. The technique requires measuring the complete state of polarization at one or more (preferably at least several) wavelengths within a magnetically sensitive line of the solar spectrum. This measurement must be done for each independent spatial point for which one wants magnetic field data. All the measurements need to be done in a time short compared to the time scale for changes of the solar features being observed. Were it possible, one would want to record all the needed data simultaneously, since temporal variation of atmospheric seeing degrades both the image and the polarization sensitivity.

Since the measurements must span four dimensions: two spatial, plus polarization and wavelength, we had some freedom to design the instrument to favor some dimensions over others in terms of simultaneity. Our earlier instrument, the Haleakala Stokes Polarimeter (Mickey 1985) records a range of wavelengths spanning two spectral lines in each reading, but requires two seconds to determine the polarization state and obtains spatial information only by assembling a long sequence (spanning an hour or two in time) of measurements at single locations on the sun. The new instrument sacrifices spectral detail and accuracy in favor of greatly improved imaging characteristics. The scientific goals for this instrument were to measure surface magnetic fields with enough accuracy to permit calculations of photospheric currents, but with a field of view covering an entire typical active region, high spatial resolution to at least match that of the X-ray telescopes now in use and to take advantage of the Haleakala site, and a fast enough temporal cadence that we can look for flare-associated changes in magnetic structures. The instrument as built has met these objectives.

Instrument Details

An instrument of this type is comprised of several identifiable subsystems, labeled by function in the block diagram of Figure 1. The particular implementation of each is described in the following paragraphs.

The image formation subsystem consists of the telescope and transfer optics. The telescope is an f:12.8 cassegrain reflector of 0.275 m aperture. A Dall-Kirkham design was chosen because its secondary is spherical and therefore easier to manufacture. Its limited field is not a problem in this application. A square field stop is located at the telescope focal plane; just ahead of the field stop a heat dump mirror diverts most of the unwanted sunlight out of the telescope. To further reduce the heat load in the system, the telescope has an entrance window with a bandpass coating which rejects nearly all the incident sunlight outside the desired 500-700 nm range. Two pairs of transfer lenses, plus a few folding mirrors and two beamsplitters, complete the basic optical system. A 60 mm diameter, 800 mm focal length achromat collimates the beam for the Fabry-Perot; an identical lens is paired with one of 120 mm focal length to reduce the beam diameter for the Rochon prism beam splitter. The two beams from the Rochon prism are imaged at the final scale of 46 μm/arcsecond by the final achromat. One image goes to the 'Data' camera by way of an order-sorting prefilter; the other is split again with part being sent to the 'Geometry' camera and the rest to the image stabilizer sensor.

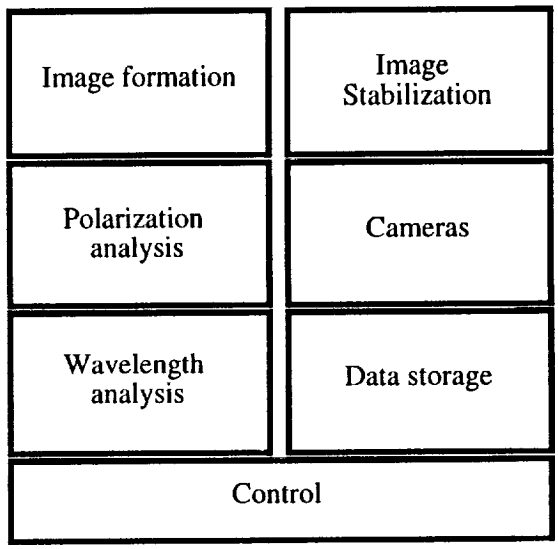

Figure 1. Functional subsystems.

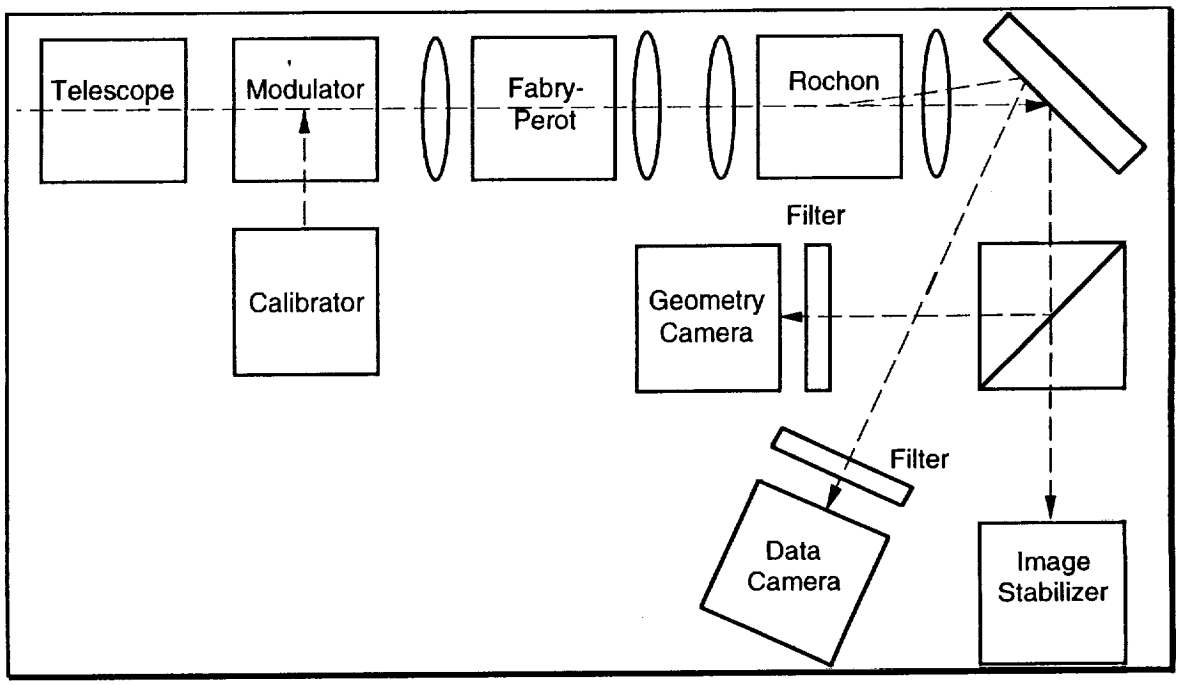

Figure 2. Optical schematic

The function of the polarization modulator is to convert polarization information into intensity differences which can be measured by the cameras. Of the various possible techniques, we have chosen to use a pair of fixed-position, variable-retardance retarders followed by a fixed polarizer. The retarders used are nematic liquid crystal devices with a retardance range of 60–2000 nm. Their retardance is controlled by varying the amplitude of a 2 kHz AC signal, in the range 3–15 volts. The advantages of this modulator design are that it has no moving parts, no high

voltages are required, and it can be tuned on millisecond time scales. Since these are true zero-order retarders, they are much less sensitive to angle of incidence than other types, so we are able to use them in an f:13 diverging beam. Two images are recorded, with the retarders at appropriate settings, to measure one polarization parameter, so six frames are required to determine the Stokes Q, U and V parameters. The brightness parameter I is obtained from the average of all six frames.

Provision has been made for polarization calibration at frequent intervals. A high-quality polarizer may be inserted in the light path ahead of the modulator, and rotated under computer control to any orientation. Sunlight is usually used, though an incandescent light source may instead be inserted ahead of the polarizer. To calibrate for circular polarization, an achromatic quarter-wave retarder is inserted following the polarizer. An automatic sequence of observations with the polarizer and retarder set to appropriate angles provides a calibration of the sensitivity to the instrument to various polarization states, and of its tendency to mix polarization states.

Wavelength selection is done by means of an air-spaced, piezo-electrically tuned Fabry-Perot etalon. The free spectral range is 0.36 nm at 630 nm; overall finesse is approximately 50 so the wavelength resolution at 630 nm is 7 pm. This is adequate to resolve the Stokes profiles of the 630.25 iron line which is used for most of our observations. The lens immediately ahead of the Fabry-Perot collimates the image, but since the ray bundle from any off-axis image point traverses the Fabry-Perot at an angle the center wavelength depends on field position. The effective wavelength shift at the extreme corners of the field is 6.1 pm relative to the center. It varies with the square of the off-axis angle, so for most of the field the variation is less than 3 pm. We have chosen to live with this variation rather than mount the Fabry-Perot in a telecentric arrangement which would remove the position-dependent variation but degrade the resolution. Since there can be 5 pm of variation in line center position, just due to motion in the solar atmosphere, we record data at up to twenty different etalon spacings and locate the line-center position separately for each pixel in the image.

Interference filters are used to select the appropriate order of the Fabry-Perot: a filter of 0.3 nm bandpass is located in front of the Data camera to select the single order used to scan the magnetically sensitive line, and a 10 nm filter in front of the Geometry camera passes about 30 orders. The geometry camera is thus essentially free from image variation due to polarization, and is used to record geometric variations due to atmospheric seeing or telescope motion.

The IVM telescope is mounted on an equatorial "spar" which tracks the sun, but the image at the IVM field stop can experience rapid motions of a few arcseconds due to telescope shake or atmospheric seeing. We have included a method of image stabilization in the instrument, since even small displacements of the image seriously corrupt the polarization measurements. Part of the beam to the Geometry camera is split off and sent to a position sensor which measures the motion of a sunspot in the field. The sensor is a lateral diffusion effect diode, which produces a voltage output proportional to the spot displacement in orthogonal directions. Provision is made for offsetting the image so we can guide on a spot anywhere within the field, and for changing the image scale on the diode to optimize performance with different spot sizes. The signals from the sensor are amplified and fed back to a fast steerable mirror (just following the Rochon prism) which stabilizes the image.

The cameras used in the IVM are commercial scientific-grade CCD cameras. The detectors are Tektronix 512×512 arrays, chosen for large well depth since photon statistics is one of the larger noise sources in the instrument. The pixel size corresponds to 0.55 arcseconds of field. The pixel readout rate is 320 kHz, so it takes about 0.8 seconds to read out the entire array. Data are digitized to twelve bits, and stored in a memory buffer until all the frames for an observation are accumulated.

Instrument control and data storage functions are implemented in a hierarchical, multi-processor computer system centered in a VMEbus crate. At the top level, the user interface and input/output functions are handled by a Sun-3 computer. The user interface is implemented in an X windows environment: a control frame on the operator's screen contains a set of buttons for single actions, plus pull-down menus providing access to subwindows with parameter entry or hardware control functions. The operator is provided with low-level access to all hardware components if needed, but the basic instrument operation can be managed with a small number of high-level commands. The X interface has the additional advantage that it permits operation from a remote site, providing there are reliable communications links. In addition to the Sun processor, a single-board 68020 computer is used for time-critical instrument control functions. A Bitbus

serial control bus provides motor control and both analog and digital interfaces. Ancillary processors are dedicated to camera control and to video acquisition and display. An attached array processor can be used for on-line data processing to provide rapid access to reduced data. A 64 MB memory board provides enough storage that a complete magnetogram can be recorded in two to four minutes, then stored to disk or tape. Magnetic disk storage is used for calibration data and daily survey magnetograms; long sequences of rapid-cadence observations are written to 8 mm tape.

Performance Characteristics

The basic observational parameters of the IVM are summarized in the following table. Most parameters can be changed according to observational goals. For example, one can increase the cadence by pixel binning, reducing the size of the field or reducing the number of wavelength points. We have made Hα polarization observations at 16 second intervals.

Field of view	280 × 280 arcsec
Pixel size	0.55 × 0.55 arcsec
Wavelength	Selectable; normally 630.25 nm
Wavelength resolution	7 pm
Magnetic field sensitivity	10 G line of sight; 200G transverse
Time resolution	Cadence depends on mode; 2–10 minutes per magnetogram

The most usual observation with this instrument is to include the full field, which encompasses an entire active region, and bin the pixels 2 × 2 so the effective pixel size is 1.1 arcseconds. We sample 20 points in the line profile, at 1.8 pm intervals, and repeat the wavelength scan twice. Every two to four hours we make dark level, flat-field and polarization calibration observations. Each magnetogram dataset is 63 MB in size. To study active region development we can make magnetograms at nine minute intervals, writing the data directly to tape.

IVM data reduction includes several steps: first the raw images are corrected for camera dark bias, then for system flat-field dependence. The geometry camera images are scanned to measure gross image motions not removed by the image stabilizer system. These residual motions are typically a few tenths of an arcsecond. The measured shifts are then used to coalign the data camera images to a precision of about 0.1 arcsecond. The data are then demodulated, converting the three pairs of intensity images into four images which correspond to the four Stokes parameters. The calibration data is reduced in the same way, then processed to determine the instrument transfer function, a 4×4 matrix for each pixel in the image, which relates the demodulated images to the true Stokes images of the incoming light. The transfer function is then used to calibrate the demodulated magnetogram data. From the calibrated Stokes spectra, the magnetic field at each pixel is derived using the "derivative" technique described by Jefferies and Mickey (Jefferies and Mickey 1991). The Stokes profiles are fit with low-order polynomials to take advantage of the line profile symmetries and utilize more of the data. We intentionally sacrifice information contained in line profile asymmetries in order to improve our determination of the mean field. The value of the fit at a selected wavelength, around three Doppler widths from line center, is used to compute the field.

We have investigated the likely sources of noise in IVM measurements. The simplest is photon statistics, i.e. the $\sqrt{N}$ uncertainty in a measurement of N photons. Our typical exposure is 2×10^5 photons per pixel and there are four frames per polarization measurement, so we would expect an uncertainty of 0.001 in the polarization measurement from this source. Electronic noise and pickup are of similar magnitude. Shutter timing jitter may also add polarization noise of 0.001, though it will be less for longer exposures. The worst source of noise is probably atmospheric seeing: small shifts and distortions of the image between the two exposures needed for a single polarization measurement. The magnitude of the "seeing noise" depends on the seeing, on the contrast in the image, and on the performance of the image stabilizer. We estimate that it typically adds 0.002 to the polarization uncertainty, but is less in the areas with low image contrast and small fields, and more around sunspots where the contrast and the fields are both larger.

Inspection of samples of quiet-sun polarization measurements support the above estimates: the variance over a frame in one polarization parameter is about 0.004, though part of that appears to have been introduced in the calibration process, since the variance of a single spatial pixel with

wavelength is only about 0.001. Histograms of the line-of-sight magnetic field indicate a detectability threshold of about 8 Gauss. The corresponding noise level in transverse field is 200 Gauss.

Figures 3 and 4 show a comparison of magnetograms obtained with the IVM and with the Haleakala Stokes Polarimeter, which has been used for magnetic field and Stokes profile observations for many years. Each figure includes a portion, chosen so the areas covered are nearly the same, of a magnetogram obtained on 1993 November 18. The gray-scale image represents the photospheric brightness and shows the locations of the spots; the contours indicate the line of sight field strength in Gauss, and the short line segments indicate the transverse field direction and—by their length—magnitude. The observed field strengths agree well. The obvious difference is the increased resolution of the IVM. Not as obvious is that these figures represent 13% of a Polarimeter scan which required 100 minutes to obtain, and 4% of an IVM scan which took four minutes.

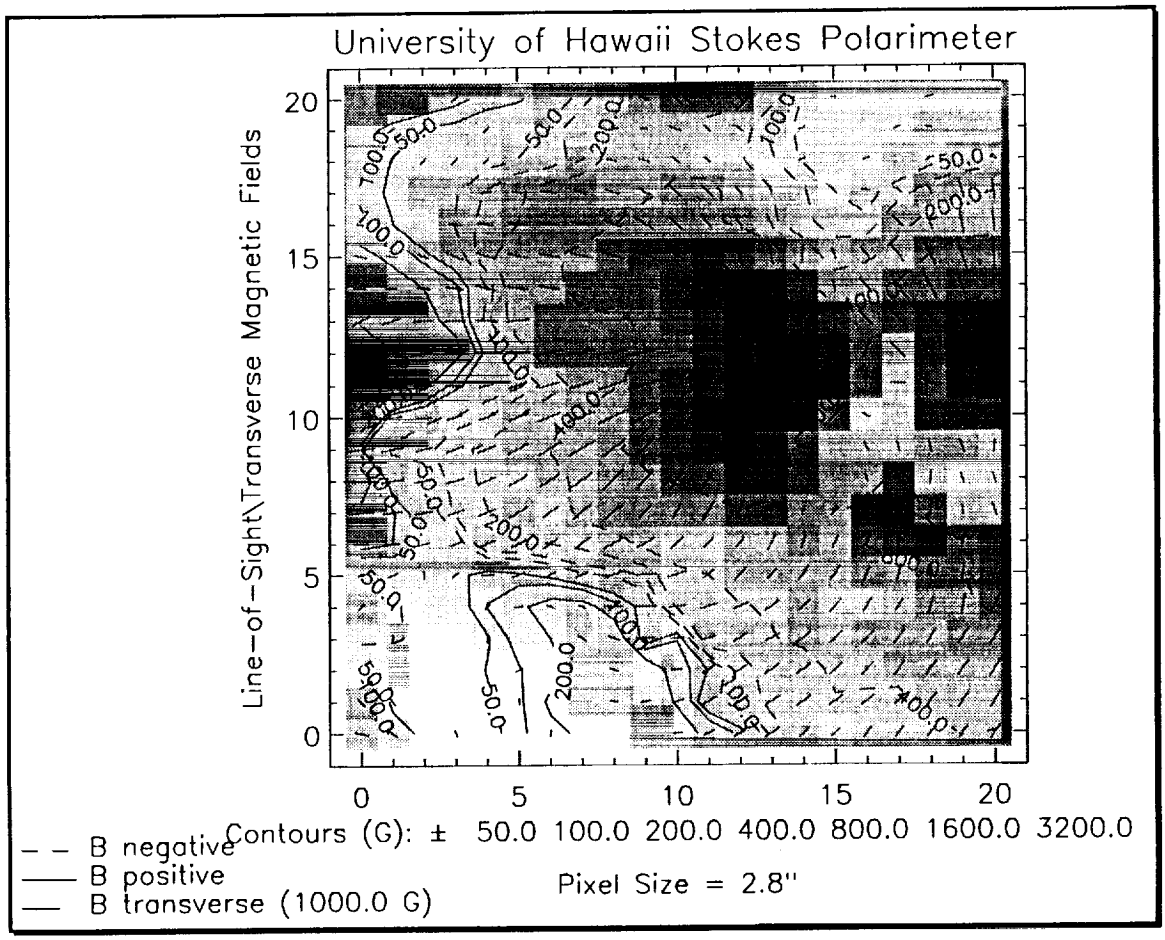

Figure 3. Polarimeter magnetogram.

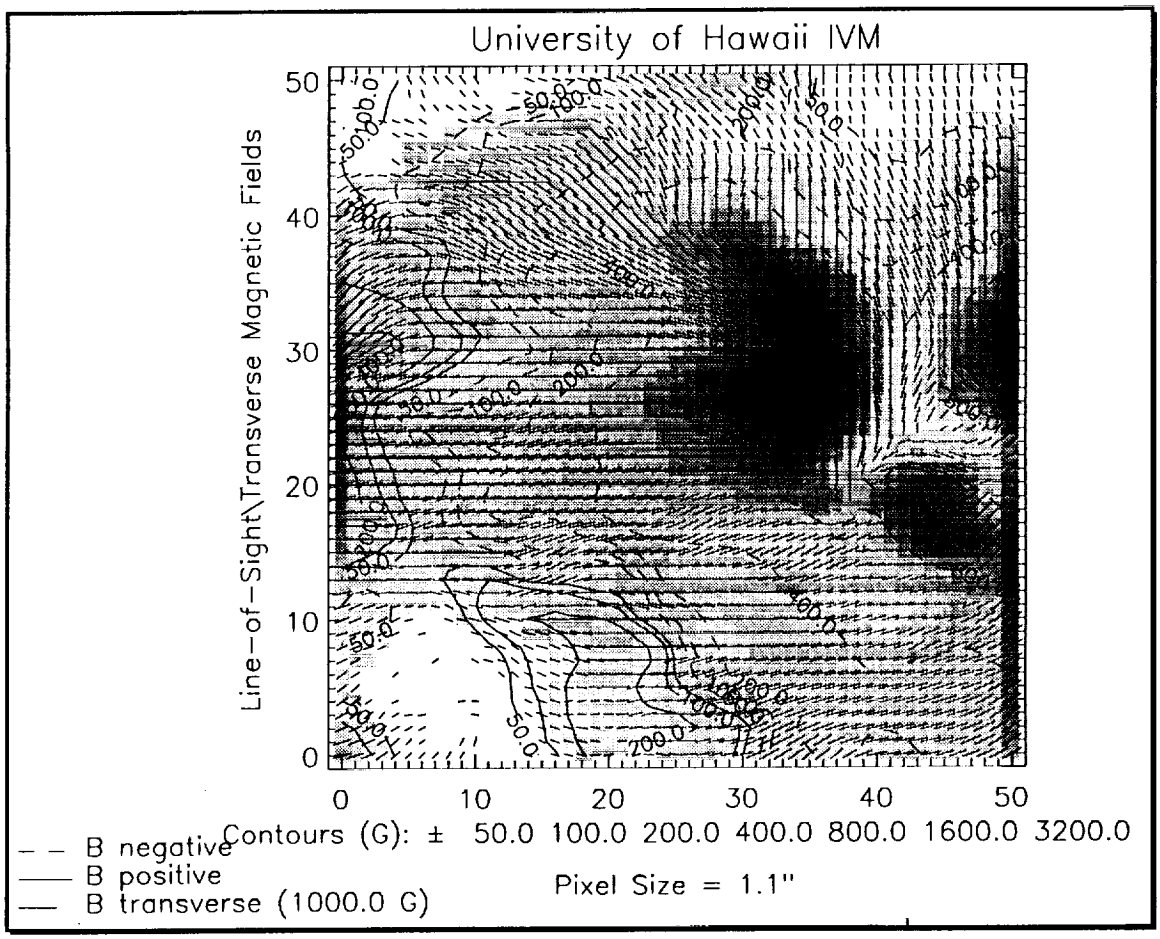

Figure 4. IVM magnetogram.

Summary

The Imaging Vector Magnetograph has been in operation since the summer of 1992, with a break during the winter of 1992–93 for optics upgrades. In 1993 it has been operated on a routine basis, obtaining up to 60 magnetograms per day in active region evolution studies. The improved spatial and temporal resolution of this instrument, compared to earlier instruments, will greatly enhance our ability to study questions of active region energy storage, sunspot growth and decay, and the connections between coronal structures and photospheric magnetic fields.

References

Jefferies, J. T. and D. L. Mickey (1991). "On the Inference of Magnetic Field Vectors from Stokes Profiles" *Astrophysical Journal* **372**: 694.

Mickey, D. L. (1985). "The Haleakala Stokes Polarimeter." *Solar Physics* **97**: 223.